Int. J. Solids Structures Vol. 28, No. 9, pp. 1155–1170, 1991
Printed in Great Britain.

0020-7683/91 $3.00 + .00

ANALYSIS OF ROTATING SOLIDS WITH CRACKS BY THE BOUNDARY ELEMENT METHOD

S. T. RAVEENDRA and P. K. BANERJEE
Department of Civil Engineering, State University of New York at Buffalo, Buffalo, NY 14260, U.S.A.

(*Received* 19 *November* 1990; *in revised form* 10 *March* 1991)

Abstract—The use of the boundary element method for the solution of linear elastic fracture mechanics problems, without body forces, is quite extensive since the method is intrinsically well suited to the analysis of high stress gradients associated with crack problems. The crack-tip stresses for rotating bodies are similar to the stresses for stationary bodies and therefore all the advantages of the boundary element procedure can be encompassed in the extension of the method to the solution of rotating bodies with cracks. In the present analysis, the additional volume integral that arises from the treatment of inertial body forces is eliminated by using the well-known particular integral procedure. The matrix ill-conditioning that results from the need to model co-planar crack surfaces of non-symmetrical cracks is avoided by using the multi-region approach. The accuracy of the numerical solutions is improved by utilizing quarter-point elements with traction singular enhancement at the crack-tip. The procedure is then applied to the solution of arbitrary cracks in two- and three-dimensional rotating bodies.

1. INTRODUCTION

Machinery with crack-like flaws, rotating at high speeds, may fail due to the weakening of flawed components. Since the strength of a cracked structural member may be characterized by the stress intensity factor (SIF), the evaluation of this parameter plays an important role in both numerical and experimental stress analyses. Investigation of rotating bodies with cracks has been performed by many investigators. For example, internal as well as edge cracks in finite rotating disks were solved by Rooke and Tweed (1972, 1973) in terms of the solution of a Fredholm integral equation; problems of cracks emanating from a central hole were solved by Owen and Griffiths (1973) and Riccardella and Bamford (1974) using the finite element method (FEM); the FEM was also used by Chen and Lin (1983) to solve arbitrary cracks in a rotating disk; Isida (1981) has used the eigenfunction expansion of the complex potentials together with the boundary collocation technique to solve internal cracks located at arbitrary positions in a disk; the method of caustics was used by Sukere (1987) to compute the stress intensity factors of internal radial cracks in rotating disks. While the boundary element method (BEM) is known to give very accurate solutions for stationary elastic bodies with cracks, it appears that the only extension of BEM to the solution of cracked rotating bodies is the application of Smith (1985), who computed stress intensity factors for arc cracks in a rotating disk. All the applications alluded to here are for two-dimensional bodies. Further, the boundary element method used by Smith utilizes a procedure which requires the evaluation of additional surface integrals. This increases the computing time considerably when compared to the solution time of the same problem without body forces.

On the other hand, in the present work, the stress intensity factors are computed using a recently-developed boundary element procedure for body forces based on particular integrals. Since the procedure does not require the evaluation of additional integrals this process is very efficient. Further, the analysis is extended for the first time for the solution of three-dimensional rotating bodies with cracks. The applicability and accuracy of this BEM procedure for the solution of rotating solids in the presence of cracks are illustrated by solving a number of two- and three-dimensional problems.

2. STRESS INTENSITY FACTORS

The near crack-tip field in a rotating body is identical in form to the corresponding field in a stationary body. The crack-tip stresses σ_{ij} due to remote loading may be expressed

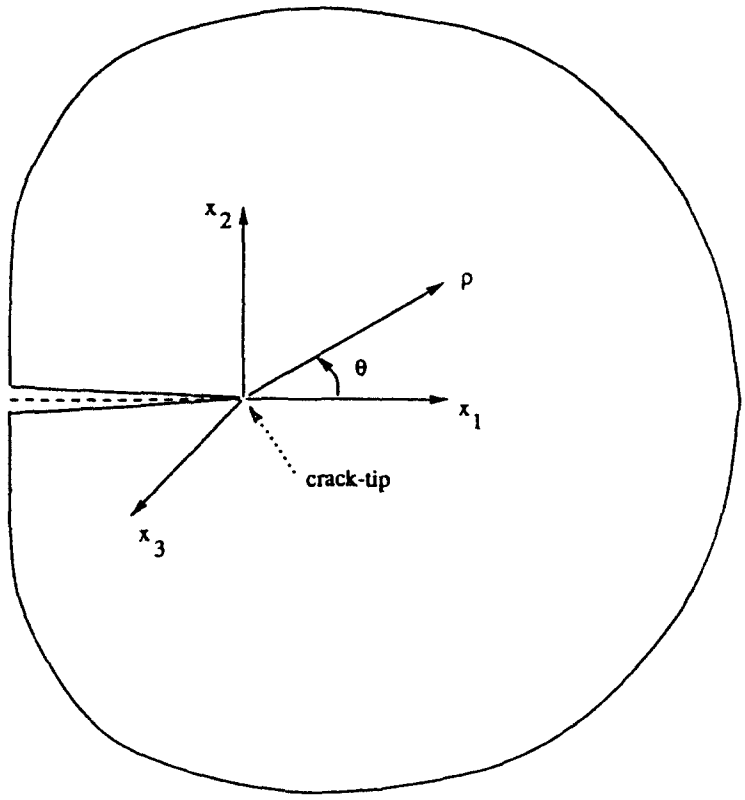

Fig. 1. Definition of crack geometry.

in terms of the distance from the crack tip ρ (see Fig. 1) as

$$\sigma_{ij} = \frac{a_{ij}^0}{\sqrt{\rho}} + a_{ij}^1 + a_{ij}^2\sqrt{\rho} + \cdots. \tag{1}$$

At the crack tip, the leading term of the stress field expression indicates the usual $1/\sqrt{\rho}$ singularity. The crack-tip stress field may also be expressed in terms of stress intensity factors (SIFs), which are defined as

$$\begin{Bmatrix} K_{\mathrm{I}} \\ K_{\mathrm{II}} \\ K_{\mathrm{III}} \end{Bmatrix} = \lim_{\rho \to 0} \sqrt{2\pi\rho} \begin{Bmatrix} \sigma_{22}|_{\theta=0} \\ \sigma_{12}|_{\theta=0} \\ \sigma_{32}|_{\theta=0} \end{Bmatrix} \tag{2}$$

where K_{I}, K_{II} and K_{III} are the mode I, mode II and mode III stress intensity factors, respectively. For a given problem, these stress intensity factors may be computed from known solutions of crack stresses using eqn (2), or from the relative opening displacements of the crack surfaces. In terms of crack opening displacements $\Delta u_i = u_i|_{\theta=\pi} - u_i|_{\theta=-\pi}$, the stress intensity factors are

$$\begin{Bmatrix} K_{\mathrm{I}} \\ K_{\mathrm{II}} \\ K_{\mathrm{III}} \end{Bmatrix} = \frac{H}{8}\sqrt{\frac{2\pi}{\rho}} \begin{Bmatrix} \Delta u_2 \\ \Delta u_1 \\ (1-\nu)\Delta u_3 \end{Bmatrix} \tag{3}$$

where, in terms of Young's modulus E and Poisson's ratio ν, $H = E$ for the plane stress case and $H = E/(1-\nu^2)$ for the plane strain and three-dimensional cases. The stresses (or tractions) and displacements required for the computation of stress intensity factors are

obtained by solving the given problem as a whole. An elegant procedure that can be used for the solution of rotating bodies with cracks is the boundary element method.

3. BOUNDARY INTEGRAL EQUATIONS FOR ROTATING BODIES

The boundary element method is well suited to the solution of elastic bodies with cracks since the method intrinsically handles high stress gradients associated with crack problems effectively. In the presence of body forces, such as the inertial force due to rotation considered in the present analysis, the integral equation for displacements $u_i(\xi)$ at a boundary point ξ may be derived using the fundamental displacement and traction solutions and the divergence theorem as

$$C_{ij}(\xi)u_i(\xi) = \int_S [G_{ij}(x,\xi)t_i(x) - F_{ij}(x,\xi)u_i(x)]\,dS(x) + \int_V G_{ij}(y,\xi)b_i(y)\,dV(y) \quad (4)$$

where $u_i(x)$ and $t_i(x)$ are the displacements and tractions at the surface S, $b_i(y)$ are the body forces within the volume V, G_{ij} and F_{ij} are the fundamental displacement and traction solutions, respectively, due to a set of unit point forces in an infinite homogeneous medium and C_{ij} are the discontinuity terms that can be evaluated indirectly using the rigid body translation of the body. A detailed derivation of eqn (4) as well as the expressions for the fundamental solutions, in both two- and three-dimensional domains, may be found in Banerjee and Butterfield (1981).

One of the major advantages of the boundary element method, for linear problems without body forces, is that the integral equations may be cast over the surface of the body only. However, for general body forces, the integral equation involves data within the problem domain, as seen by eqn (4). Nevertheless, the volume integral due to inertial body forces may be converted to equivalent surface integrals. Cruse and Wilson (1977) and Rizzo and Shippy (1977) have used the field equations due to inertial potential and the divergence theorem to convert the volume integral to equivalent surface integrals. This procedure was used by Smith (1985) to compute stress intensity factors of arc cracks in rotating disks. However, this procedure requires the evaluation of additional surface integrals that arise from the transformation of the volume integral to surface integrals. This can be avoided by using the well-known particular integrals procedure tentatively discussed in the context of boundary element method by Jaswon and Maiti (1968) and used previously by Pape and Banerjee (1987) and Banerjee *et al.* (1988), among others.

To illustrate the particular integral procedure, consider the governing differential equations for the deformation of a homogeneous body rotating about a fixed axis through the origin of coordinates. The equations may be expressed in terms of shear modulus μ, Poisson's ratio ν, density ρ and angular velocity ω as

$$(\lambda+\mu)\frac{\partial^2 u_j}{\partial x_i\,\partial x_j} + \mu\frac{\partial^2 u_i}{\partial x_j\,\partial x_j} + \rho\omega^2 x_i = 0 \quad (5)$$

where $\lambda = 2\nu\mu/(1-2\nu)$.

Let u_i^p be a set of displacement particular solutions of the above governing differential equations. Using the fundamental solutions and the divergence theorem, an integral equation corresponding to the particular solution field may be derived as

$$C_{ij}(\xi)u_i^p(\xi) = \int_S [G_{ij}(x,\xi)t_i^p(x) - F_{ij}(x,\xi)u_i^p(x)]\,dS(x) + \int_V G_{ij}(y,\xi)b_i(y)\,dV(y) \quad (6)$$

where t_i^p are the traction particular solutions and $b_i = \rho\omega^2 x_i$. The volume integral in eqn (4) is then eliminated by deducting eqn (6) from (4) to arrive at

$$C_{ij}(\xi)\hat{u}_i(\xi) = \int_S [G_{ij}(x,\xi)\hat{t}_i(x) - F_{ij}(x,\xi)\hat{u}_i(x)]\,dS(x) \quad (7)$$

where

$$\hat{u}_i = u_i - u_i^p$$
$$\hat{t}_i = t_i - t_i^p. \tag{8}$$

The form of the above equation is identical to the corresponding integral equation for the same problem without body forces, except that eqn (7) requires the knowledge of both actual and particular displacement and traction fields. Therefore, for known particular integrals, the solution of eqn (7) is similar to the solution of a problem without body forces which is rather straightforward.

4. PARTICULAR SOLUTIONS

For a two-dimensional body, rotating about a fixed axis perpendicular to the plane of the body through the origin, the displacement particular solutions of eqn (5) are given by Sokolnikoff (1956) as

$$u_\alpha^p = -\frac{\rho\omega^2}{8(\lambda+2\mu)} x_\beta x_\beta x_\alpha, \quad \alpha, \beta = 1, 2. \tag{9}$$

Similarly, for a three-dimensional body, rotating about the x_3-axis, the displacement particular solutions are given by Banerjee *et al.* (1988) as

$$u_\alpha^p = -\frac{\rho\omega^2}{8(\lambda+2\mu)}\left[\frac{5\lambda+4\mu}{4(\lambda+\mu)} x_\beta x_\beta + \frac{\mu}{\lambda+\mu} x_3^2\right] x_\alpha$$
$$u_3^p = \frac{\rho\omega^2}{8(\lambda+2\mu)} x_\beta x_\beta x_3. \tag{10}$$

The required traction particular solutions are then calculated by using the constitutive law and Cauchy relationship.

These particular solutions, while not unique, exactly satisfy the governing inhomogeneous differential equations. However, any solution to the homogeneous equations can be added to these particular solutions to form a new set of particular solutions that satisfy the inhomogeneous equations. Nevertheless, the final solution is entirely independent of the particular integrals used, provided the chosen particular solutions can be represented acceptably by the interpolation functions that are used for the approximation of displacements and traction fields within each element. Therefore, generally, a basic form of the particular solutions such as the one given by eqns (9) and (10) is used to minimize the computing effort.

5. BOUNDARY ELEMENT PROCEDURE FOR FRACTURE MECHANICS

The numerical solution of the boundary integral equation is facilitated by approximating the surface of the body by a finite number of boundary elements and interpolating displacements and tractions within each element by shape functions in terms of nodal values. Generally, accurate solutions may be obtained by using quadratic shape functions for the approximation of both geometry and field variables. However, in crack problems, the accuracy of the solution depends considerably on how well the displacements and tractions are represented in the vicinity of the crack tip. The generally used quadratic shape functions provide neither the correct singular representation of the stress field nor the $\sqrt{\rho}$ variation of the displacement field. It is well established by Barsoum (1976) in FEM and Cruse and Wilson (1977) in BEM that by placing the mid-nodes at geometric quarter points for the sides emanating from the crack, as shown in Fig. 2, the variation of crack opening

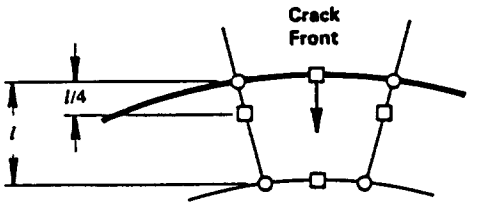

Fig. 2. Typical crack-tip quarter-point element.

displacements is constricted to an asymptotic $\sqrt{\rho}$ behavior as

$$\{u(\rho)\} = A_1 + A_2\sqrt{\frac{\rho}{l}} + A_3\frac{\rho}{l} \tag{11}$$

where A_i are functions of nodal displacements and l is the element length. Since the tractions are also approximated by the same interpolations, to simulate the correct singular behavior of stresses, the nominal tractions $\hat{t}_i$ obtained from the quarter-point modeling are multiplied by a non-dimensional parameter $\sqrt{(l/\rho)}$ such that

$$\{t(\rho)\} = \sqrt{\frac{l}{\rho}}\cdot\{\hat{t}(\rho)\} = B_1\sqrt{\frac{l}{\rho}} + B_2 + B_3\sqrt{\frac{\rho}{l}} \tag{12}$$

where B_i are the nodal tractions. The use of quarter-point (QP) elements, for the first row of elements behind the crack front, and QP elements with traction singular (TS) modification, for the first row elements ahead of the crack front, improves the accuracy of the BEM solutions considerably as seen by the numerical examples provided later in this text.

It should be noted that unless the problem geometry and loading are symmetrical with respect to the crack the BEM procedure requires the modeling of co-planar surfaces of the crack. The numerical solution of non-symmetrical crack problems, by applying the integral equation directly, is not viable due to the ill-conditioning of the matrix that results from the modeling of co-planar crack surfaces. A general modeling approach which is effective for the solution of non-symmetric cracks is the multi-region approach utilized by Blandford *et al.* (1981). In the multi-region approach, the body is divided into sub-regions along the crack surface and the integral equation is applied independently for each region. The final solution is then obtained by coupling the equations from each region using the compatibility of displacements and continuity of tractions along the interface of jointed regions. The multi-region approach not only avoids the ill-conditioning of the matrix but also improves the solution accuracy and efficiency. The presence of inertial forces does not pose any additional problem in the multi-region approach since the contribution of the body force is accounted for via known particular solutions.

6. COMPUTATION OF STRESS INTENSITY FACTORS

The displacements and tractions obtained from the boundary element method can be used together with eqns (2) and/or (3) to compute the stress intensity factors. It should be noted that although the tractions t_i^0 at the crack-tip are unbounded, the nominal tractions $\hat{t}_i^0$ are finite since from eqn (12) as $\rho \to 0$

$$\{\hat{t}^0\} = \sqrt{\frac{\rho}{l}}\cdot\{t^0\} = B_1. \tag{13}$$

Using eqns (2) and (13) together with the relationship between stresses and tractions, the

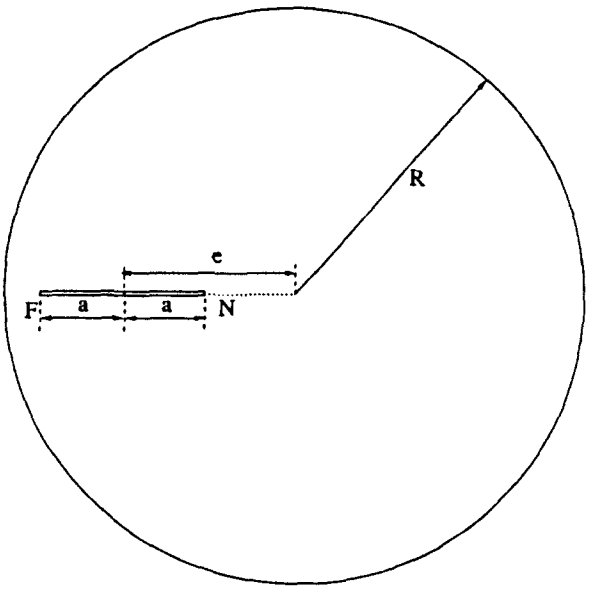

Fig. 3. Geometry of a radial crack in a rotating disk.

stress intensity factors can be computed from the crack-tip nominal tractions as

$$\begin{Bmatrix} K_I \\ K_{II} \\ K_{III} \end{Bmatrix} = \sqrt{2\pi l} \begin{Bmatrix} \hat{t}_2^0 \\ \hat{t}_1^0 \\ \hat{t}_3^0 \end{Bmatrix}. \tag{14}$$

Alternatively, the stress intensity factors may also be computed from the crack-opening displacements using eqn (3). Comparing the stress intensity factors based on tractions and displacements it is found, in the current analysis, that the values using tractions depend very much on the accuracy of the numerical integration scheme used for the evaluation of the higher-order singular integrals† involving modified tractions at the crack front elements. On the other hand, the overall solution as well as the crack-opening displacements are less sensitive to the accuracy of this integration and therefore the stress intensity factors in the current analysis are computed from the crack-opening displacements using eqn (3).

7. NUMERICAL EXAMPLES

To validate the analysis and to assess the accuracy of the numerical procedure, an arbitrarily-located crack in a rotating disk is studied. The location and the dimension of the crack are fixed by $\varepsilon = \lambda = 0.5$, where ε and λ are normalized eccentricity and length parameters, respectively, defined in terms of the problem geometry shown in Fig. 3 as

$$\varepsilon = e/R$$

$$\lambda = \frac{a}{(R-e)}.$$

† The singularity of the kernel to be integrated is increased since using eqn (13),

$$\int_S G_{ij} t_j \, dS = \int_S G_{ij} \sqrt{\frac{l}{\rho}} \hat{t}_j \, dS = \int_S \hat{G}_{ij} \hat{t}_{ij} \, dS \quad \text{where} \quad \hat{G}_{ij} = G_{ij} \cdot \sqrt{\frac{l}{\rho}}.$$

Therefore, the singularity of $\hat{G}_{ij}$ is higher than that of G_{ij}. This additional singularity may be removed by a simple change of variable such as $\hat{\rho}^2 = \rho$.

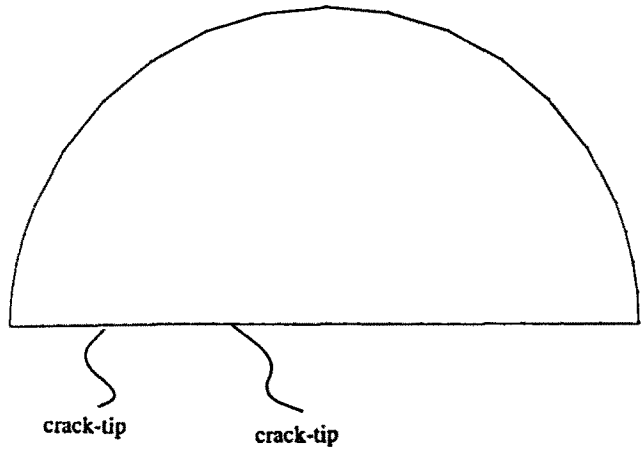

Fig. 4. Boundary element model for a radial crack.

Due to symmetry, only one half of the disk is modeled, as shown in Fig. 4. The stress intensity factors are calculated at both crack tips. These SIFs are normalized with respect to $\sigma_0\sqrt{\pi a}$, where σ_0 is the stress at the center of an uncracked rotating disk. The radial σ_r and hoop σ_θ stresses in an uncracked disk of density ρ and Poisson's ratio ν, rotating at an angular velocity of ω about an axis through the center, are given by Love (1944) as

$$\sigma_r = \frac{\rho\omega^2}{8}(3+\nu)(R^2-r^2)$$

$$\sigma_\theta = \frac{\rho\omega^2}{8}\{(3+\nu)R^2-(1+3\nu)r^2\}.$$

At the center of the crack both radial and hoop stresses reduce to $\sigma_0 = (3+\nu)\rho\omega^2R^2/8$. The normalized stress intensity factors $\hat{K}_{I,N}$ and $\hat{K}_{I,F}$ at the near (N) and far (F) ends from the center of the disk are compared in Table 1 to the corresponding solutions of Isida (1981), who computed the stress intensity factors using the eigenfunction expansion of complex potentials together with the boundary collocation technique. Three BEM models are used: in the first model, regular quadratic elements are used everywhere, in the second model, elements next to the crack tips on both sides are replaced by quarter-point (QP) elements, and in the final model, QP elements ahead of the crack tips are enhanced by traction singular (TS) modification. In all three cases, one half of the crack is modeled by using three boundary elements, the size of the crack-tip element is 5% of the crack length and the second and third elements are 20% and 25%, respectively, of the crack length. The reported results show that the solutions using QP elements with TS modification are within 1% of the solutions given by Isida, which are considered to be correct up to the last figures except for rounding errors.

Table 1. Mode I stress intensity factor for various crack-tip elements

	Isida	BEM		
		Regular	QP	QP & TS
$\hat{K}_{I,N}$	1.0362	1.0719	0.9973	1.0270
% DIFF		−3.4	3.8	0.9
$\hat{K}_{I,F}$	0.9404	0.9865	0.9049	0.9344
% DIFF		−4.9	3.8	0.6

% DIFF = 100 $[\hat{K}(\text{BEM}) - \hat{K}(\text{Isida})/\hat{K}(\text{Isida})]$.

Having established the validity and accuracy of the solution procedure, the remainder of the numerical analyses are performed using QP and TS elements at the crack tips. The disk shown in Fig. 3 is analyzed further by changing the location and size of the crack. The normalized SIFs computed by the BEM at both crack tips for arbitrary crack length parameter λ at eccentricities ε are compared in Figs 5 and 6 to the results of Isida. In addition to the excellent agreement between the present solutions and the eigenfunction

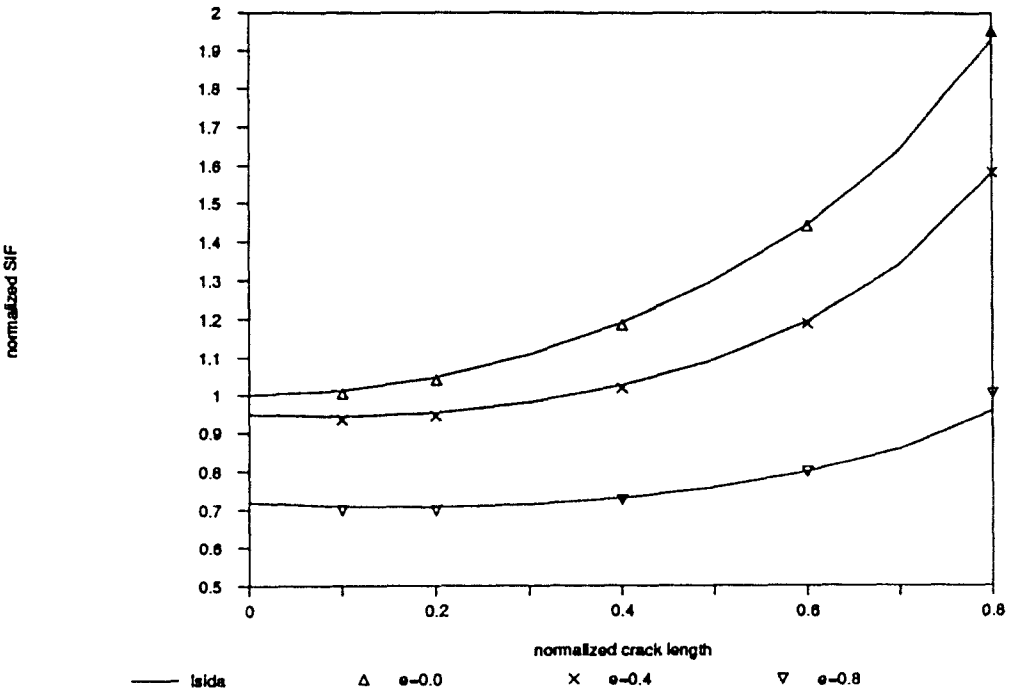

Fig. 5. Comparison of mode I SIFs at the crack tip F.

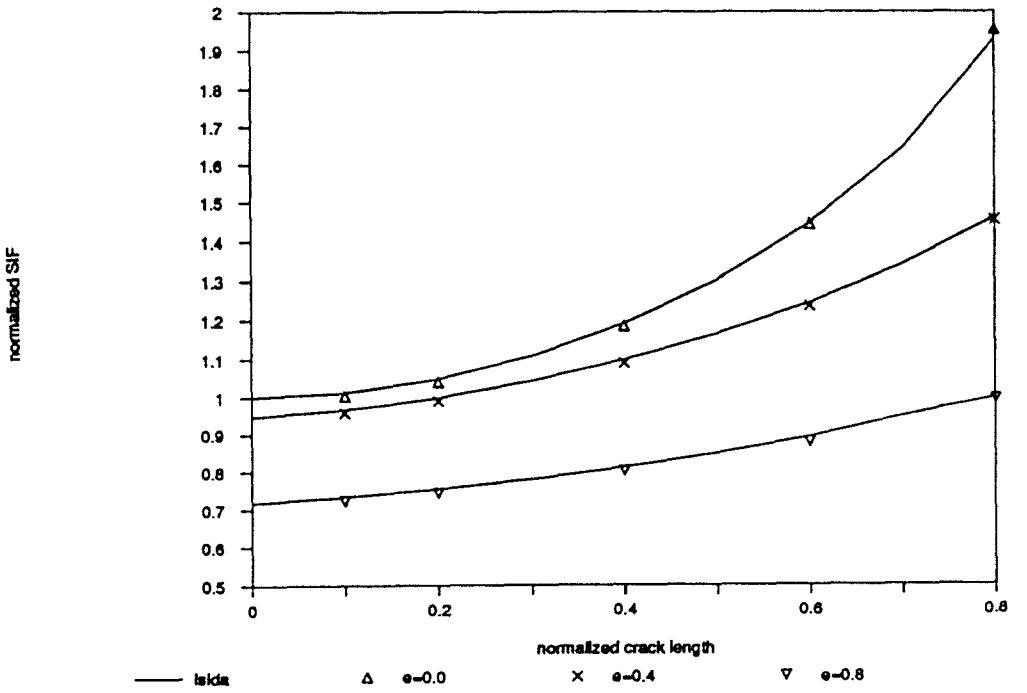

Fig. 6. Comparison of mode I SIFs at the crack tip N.

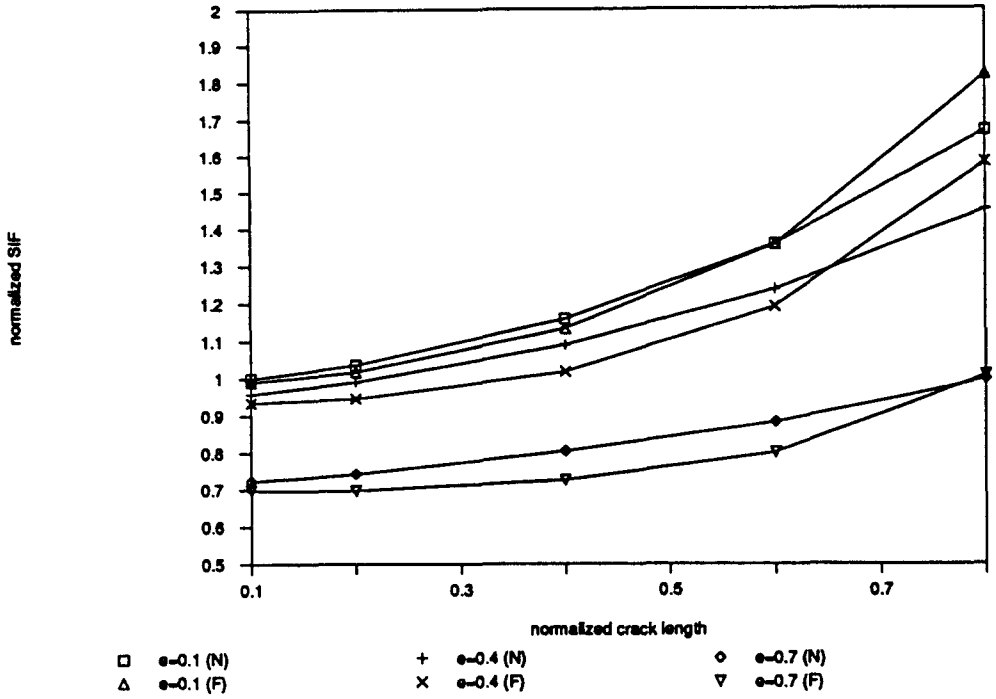

Fig. 7. Mode I SIFs at both crack tips for radial cracks.

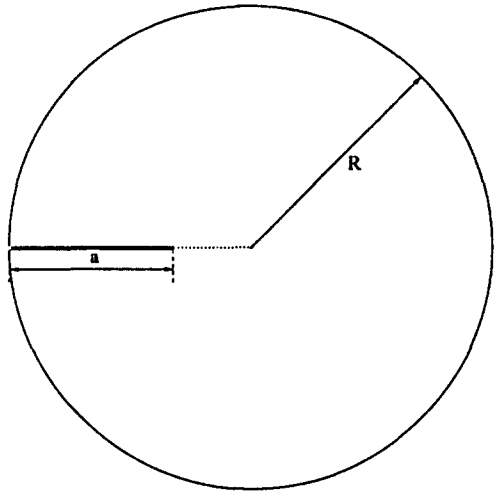

Fig. 8. Geometry of an edge crack in a rotating disk.

method results, the figures show that the normalized stress intensity factors increase with crack length at both crack tips. Further, the results for both ends of the cracks plotted together in Fig. 7 indicate that while the normalized stress intensity factors at the crack tip closer to the disk center are larger than the corresponding factors at the other end for small values of length parameter λ, the trend is reversed at large values of λ.

The second example examined is the problem of an edge crack in a cylinder under plane strain condition studied previously by Schneider and Danzer (1989) using the weight function method. Figures 8 and 9 show the geometry of the problem and the boundary element map of one half of the disk. The BEM and weight function method stress intensity factor solutions normalized as in the previous example†, compared in Fig. 10, show that

† Note that the stress at the center of the uncracked body, under plane strain condition, is obtained from the previously defined plane stress expression of $\sigma_0 = (3+\hat{\nu})\rho\omega^2 R^2/8$ by replacing $\hat{\nu}$ by $\nu/(1-\nu)$.

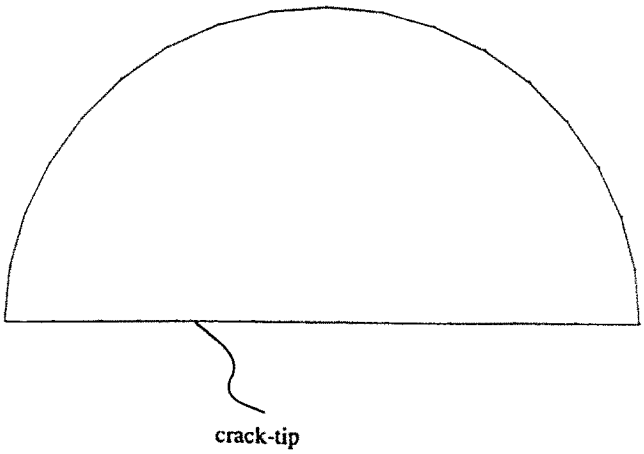

Fig. 9. Boundary element model for an edge crack.

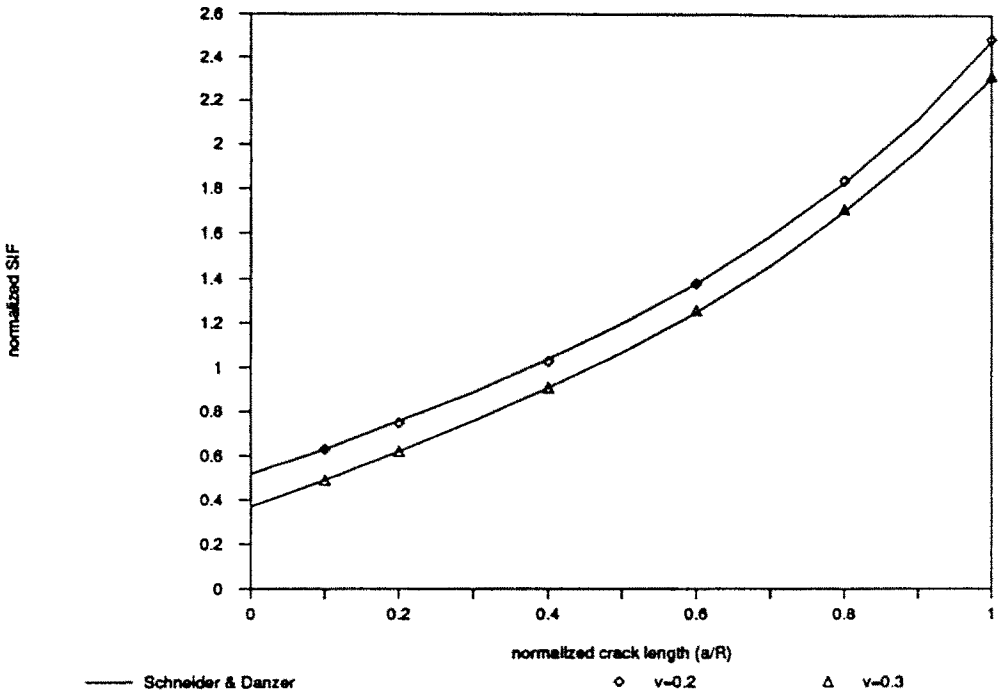

Fig. 10. Comparison of mode I SIFs for edge cracks.

the agreement between the results is excellent. The results in Fig. 10 are for two different values of ν to indicate the dependence of stress intensity factors on the Poisson's ratio, which is apparently not elaborated in the cited reference.

Mixed-mode crack problems are studied by computing the stress intensity factors of arc cracks in a rotating disk. The problem geometry and BEM model of one half of the disk are shown in Figs 11 and 12, respectively. Since the geometry and loading are not symmetrical with respect to the crack, the half disk is modeled as a two-region problem. The mode I and mode II stress intensity factors are normalized with respect to $\sigma_0\sqrt{\pi r}\sin\theta$, where σ_0 is the radial stress of the uncracked rotating body at a radius of r given by $\sigma_0 = (3+\nu)\rho\omega^2(R^2-r^2)/8$. The BEM results are compared in Figs 13 and 14 to the corresponding solutions obtained by Smith (1985), who used an alternative BEM formulation based on transforming the volume integral involving inertial body forces to equivalent surface integrals. The results show excellent agreement between different BEM formu-

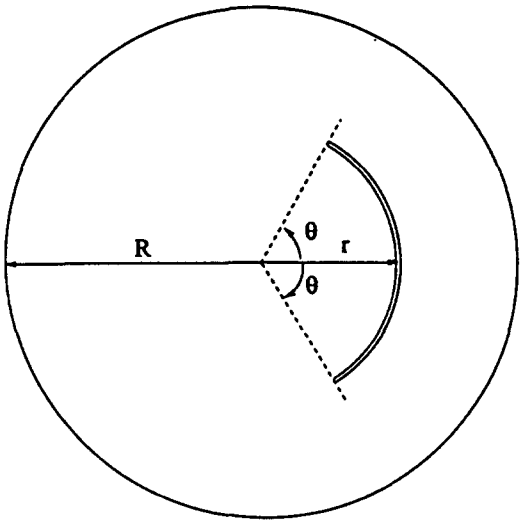

Fig. 11. Geometry of an arc crack in a rotating disk.

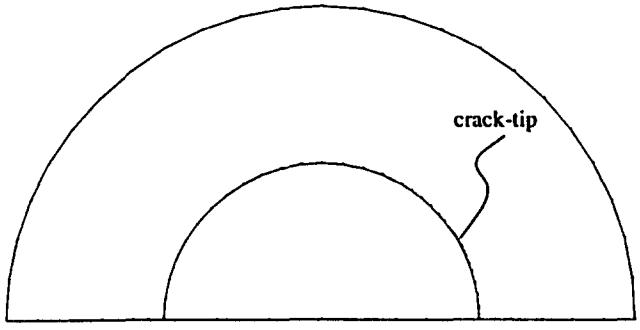

Fig. 12. Multi-region boundary element model for an arc crack.

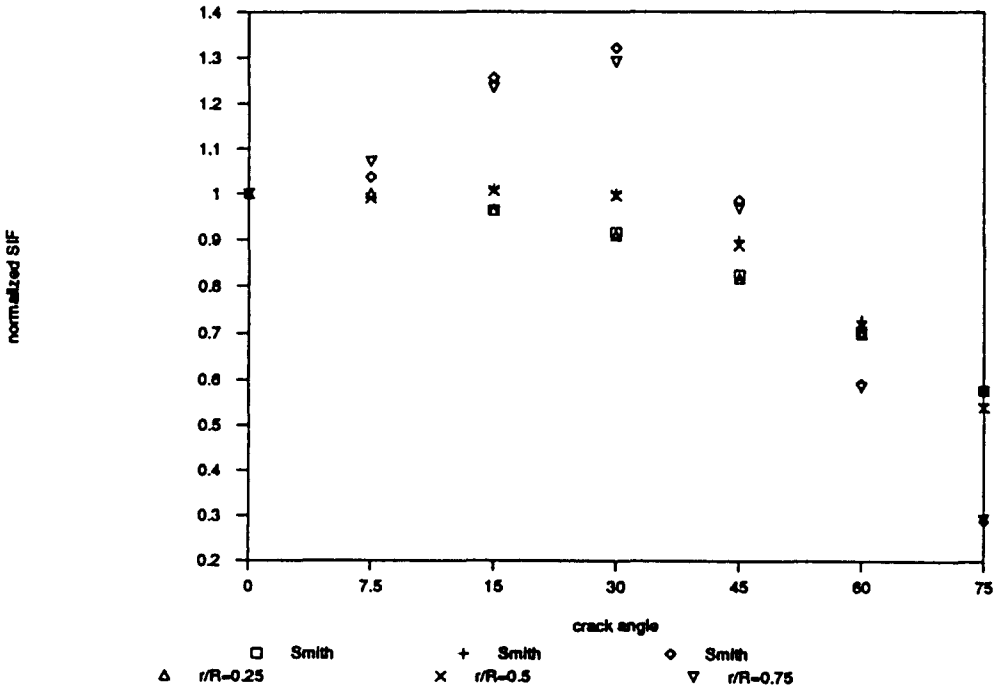

Fig. 13. Comparison of mode I SIFs for arc cracks.

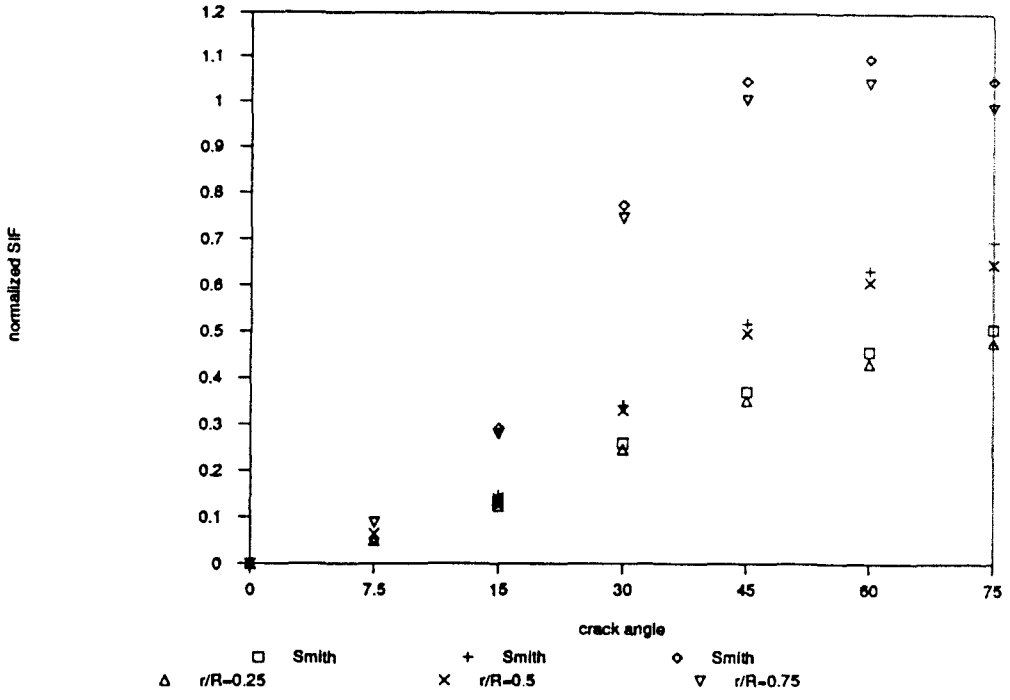

Fig. 14. Comparison of mode II SIFs for arc cracks.

lations, however, the computing time for the present formulation is notably less than the time required for the formulation used by Smith.

The three-dimensional BEM procedure for rotating bodies with cracks is validated by comparing the solution of a rectangular through crack in a cylinder to the corresponding two-dimensional plane strain result. The problem geometry is shown in Fig. 15 and the boundary element model of one quarter of the cylinder for a typical crack length is shown in Fig. 16. The mode I stress intensity factors computed at various depths are compared to the plane strain solutions in Fig. 17. The stress intensity factors and crack lengths are normalized with respect to the same parameters as in example 2. The results indicate that the mode I solutions at various depths remain the same and are in agreement with the plane strain solutions, as expected. The results further show that the normalized stress intensity factors increase with crack length. It should be noted that the stress intensity factors for the three-dimensional case at all locations are computed by using the plane strain expression given by eqn (3) and therefore the true three-dimensional surface effect is not reflected by these results.

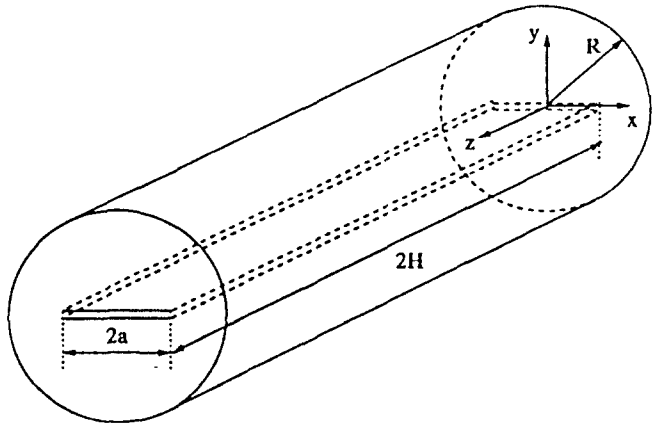

Fig. 15. Geometry of a cylinder with a through crack.

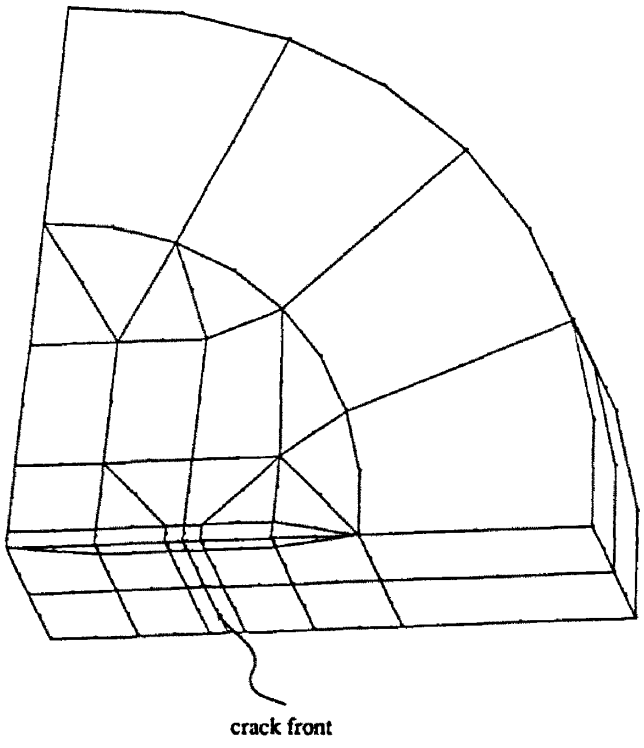

Fig. 16. Boundary element model for a cylinder with a through crack.

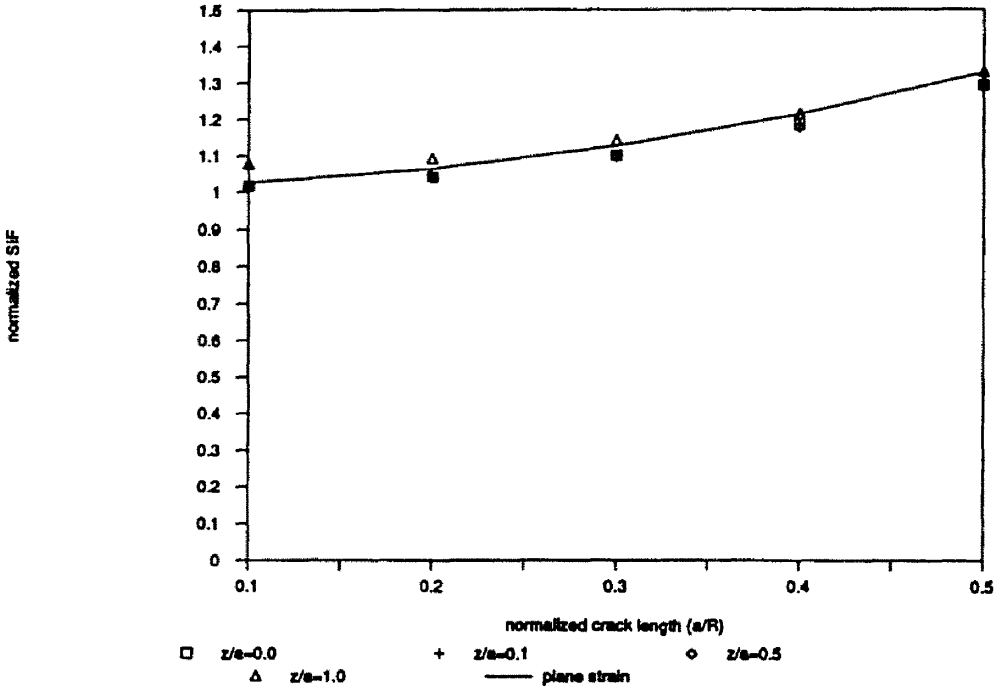

Fig. 17. Comparison of mode I SIFs to plane strain results.

The next example investigated is the problem of a circular crack embedded in a finite cylinder. Figures 18 and 19 show the problem geometry and the boundary element map of one quarter of the body, respectively. The problem is studied under two conditions: in the first case the cylinder is restrained at both ends, thus simulating the plane strain condition

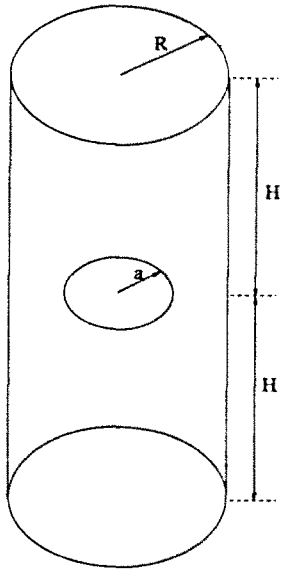

Fig. 18. Geometry of a buried circular crack in a finite cylinder.

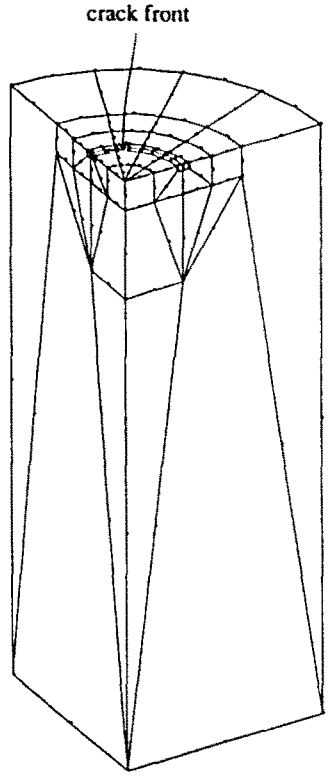

Fig. 19. Boundary element model for a circular crack.

and in the second case the cylinder is free at both ends. The analytical results for stresses in an uncracked rotating cylinder under plane strain condition are the same as the previously-reported expressions for a rotating disk with modified ν. Moreover, under plane strain condition, the out-of-plane stress σ_z is

$$\sigma_z = \frac{\rho\omega^2}{4}\frac{\nu}{1-\nu}[(3-2\nu)R^2 - 2r^2].$$

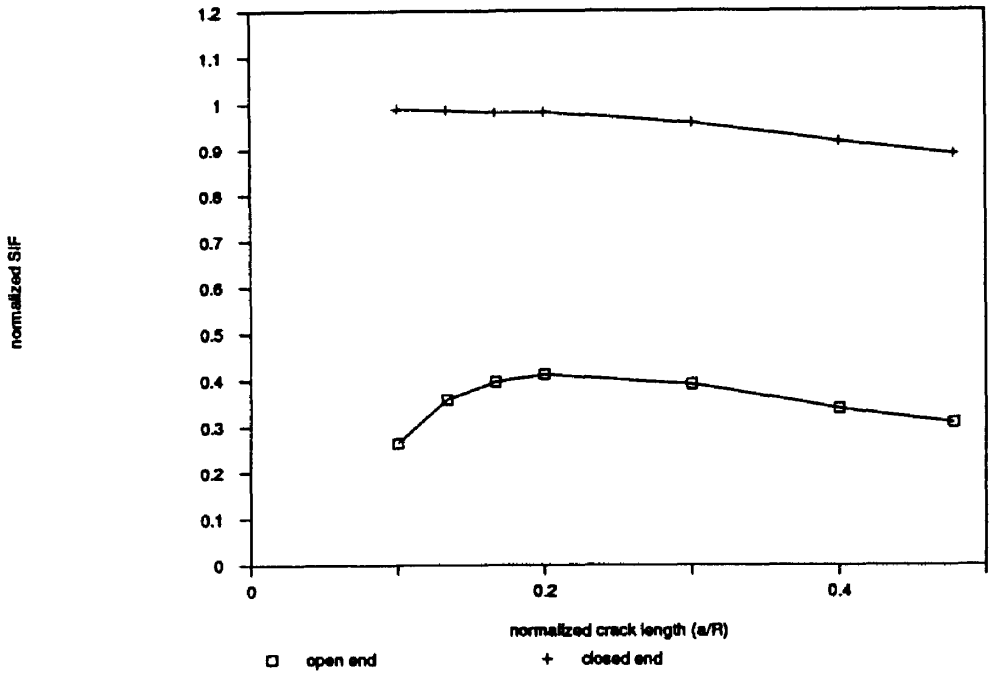

Fig. 20. Mode I SIFs for embedded circular cracks.

The mode I stress intensity factors computed are normalized with respect to the SIF K_I^S of the corresponding stationary crack problem subjected to a uniform crack surface stress of σ_0, where

$$K_I^S = 2\sigma_0\sqrt{\frac{a}{\pi}}$$

$$\sigma_0 = \sigma_z|_{r=0} = \frac{\rho\omega^2}{4}\frac{\nu}{1-\nu}(3-2\nu)R^2.$$

The normalized stress intensity factors for different crack sizes, computed for fixed and free ends, are plotted in Fig. 20. Under plane strain simulated condition, the normalized stress intensity factors for small cracks are expected to have a magnitude of 1. This is due to the fact that the SIFs are normalized with respect to the out-of-plane stress at the center, which is approximately equal to the stress at the crack surface for small cracks. The stress intensity factors, however, decrease with increasing crack length since the magnitude of the difference between σ_0 and σ_z increases with crack length. On the other hand, the normalized SIFs under free-end condition increase at small values of crack size but decrease at large crack sizes.

8. CONCLUSIONS

The boundary element method is extended for the solution of cracks in rotating two- and three-dimensional bodies. The volume integral associated with the inertial force is eliminated by using the particular integral procedure. This solution procedure is very efficient compared to the transformation procedure which converts the volume integral due to the inertial force to equivalent surface integrals. The modeling of the crack-tip field is improved by employing quarter-point elements with traction singular enhancement at the crack tips. The excellent agreement between the present solutions and the results available in the literature for two-dimensional problems confirms the validity and applicability of the current solution technique. The procedure is then extended to solve three-dimensional

problems. The increase in solution times for all cases is, typically, less than 10% of the corresponding solution times for stationary crack problems, thereby highlighting the desirability of the current procedure as a practical tool for the solution of crack problems in rotating bodies.

REFERENCES

Banerjee, P. K. and Butterfield, R. (1981). *Boundary Element Methods in Engineering Science*. McGraw-Hill, London.

Banerjee, P. K., Wilson, R. B. and Miller, N. (1988). Advanced elastic and inelastic three-dimensional analysis of gas turbine engine structures by BEM. *Int. J. Numer. Engng* **26**, 393–411.

Barsoum, R. S. (1976). On the use of isoparametric finite elements in linear fracture mechanics. *Int. J. Numer. Methods Engng* **10**, 25–37.

Blandford, G. E., Ingrafea, A. R. and Ligget, J. A. (1981). Two-dimensional stress intensity factor computations using the boundary element method. *Int. J. Numer. Methods Engng* **17**, 387–404.

Chen, W. H. and Lin, T. C. (1983). A mixed-mode crack analysis of rotating disk using FEM. *Engng Frac. Mech.* 18(1), 133–143.

Cruse, T. A. and Wilson, R. B. (1977). Boundary element methods for elastic fracture mechanics. AFORSR-TR-78-0355, Accession No. ADA 051992.

Isida, M. (1981). Rotating disk containing an internal crack located at an arbitrary position. *Engng Frac. Mech.* **14**, 549–555.

Jaswon, M. A. and Maiti, M. (1968). An integral equation formulation for plate bending problems. *J. Engng Math.* **2**, 83–90.

Love, A. E. H. (1944). *A Treatise on the Mathematical Theory of Elasticity*. Dover, New York.

Owen, D. R. J. and Griffiths, J. R. (1973). Stress intensity factors of cracks in a plate containing a hole and in a spinning disc. *Int. J. Fracture* **9**, 471–476.

Pape, D. A. and Banerjee, P. K. (1987). Treatment of body forces in 2D elastostatic BEM using particular integrals. *J. Appl. Mech. ASME* **54**, 866–871.

Riccardella, P. C. and Bamford, W. H. (1974). Reactor coolant pump flywheel overspeed evaluation. *J. Press. Vess. Technol. ASME* **96**(4), 279–285.

Rizzo, F. J. and Shippy, D. J. (1977). An advanced integral equation method for three-dimensional thermoelasticity. *Int. J. Numer. Engng* **11**, 1753–1768.

Rooke, D. P. and Tweed, J. (1972). The stress intensity factors of a radial crack in a finite rotating elastic disc. *Int. J. Engng Sci.* **10**, 709–714.

Schneider, G. A. and Danzer, R. (1989). Calculation of the stress intensity factor of an edge crack in a finite elastic disc using the weight function method. *Engng Frac. Mech.* **34**(3), 547–552.

Smith, R. N. L. (1985). Stress intensity factors for an arc crack in a rotating disc. *Engng Frac. Mech.* **21**(3), 579–587.

Sokolnikoff, I. S. (1956). *Mathematical Theory of Elasticity*, 2nd Edn. McGraw-Hill, New York.

Sukere, A. A. (1987). The stress intensity factors of internal radial cracks in rotating disks by the method of caustics. *Engng Frac. Mech.* **26**(1), 65–74.